

## Surface Studies of Chromate Binding to Fused Quartz/Water Interfaces

Amanda L. Mifflin, Katie A. Gerth, Brian M. Weiss,<sup>†</sup> and Franz M. Geiger\*

Department of Chemistry, Northwestern University, 2145 Sheridan Road, Evanston, Illinois 60208

Received: February 5, 2003; In Final Form: June 5, 2003

While it is well known that chromium contamination in groundwater represents a considerable threat to the environment, little is known about the heterogeneous processes that govern chromium interaction with solid materials in soil. Using the nonlinear optical laser spectroscopy surface second harmonic generation (SHG), we have studied chromate adsorption and desorption at the fused quartz/liquid water interface in real time, at room temperature and at chromate concentrations between  $1 \times 10^{-6}$  and  $2 \times 10^{-4}$  M. Adsorbed chromate is spectroscopically identified via a two-photon resonance of one of its ligand-to-metal charge-transfer bands with the fundamental probe light. Adsorption isotherm measurements at 300 K result in a free chromate adsorption energy  $\Delta G_{\text{ads}}$  of  $38 \pm 1$  kJ/mol at pH 7. Real-time kinetic measurements of chromate adsorption and desorption show reversible chromate binding to the fused quartz/water interface, consistent with the high mobility of Cr(VI) in soils and the  $\Delta G_{\text{ads}}$  determined from our adsorption isotherm measurements. The pH dependence of chromate binding to the fused quartz/water interface is discussed.

### I. Introduction

Among toxic metal contaminants, chromium is second in abundance after lead<sup>1</sup> and originates mainly from fossil fuel combustion, metal, alloy, and wood industries, and petrochemical cooling towers.<sup>2–6</sup> Cr(III) and Cr(VI) (in the form of chromate,  $\text{CrO}_4^{2-}$ ) are the two stable oxidation states in the environment,<sup>7</sup> with Cr(VI) contamination being almost entirely anthropogenic.<sup>8,9</sup> Cr(VI) carcinogenicity, toxicity,<sup>5,8,10–14</sup> and high mobility<sup>8,15–21</sup> in soils causes great environmental concern. In contrast, Cr(III) occurs naturally, is less mobile than Cr(VI) and, in small quantities, is an essential trace element for humans and animals.<sup>5,8</sup> Certain oxides and organic compounds are known to convert Cr(III) back to Cr(VI), and the recognition of this type of redox chemistry has led to the assessment that all chromium compounds are potentially carcinogenic.<sup>8,22</sup>

In general, binding and heterogeneous transformations of chromium species in the environment are governed by surface mechanisms.<sup>23</sup> Modern groundwater pollutant transport models rely on pollutant-to-soil binding constants that depend on pollutant adsorption and desorption rate constants.<sup>23</sup> An understanding of chromium binding to mineral surfaces is tightly linked to predicting migration potentials of heavy metal ions and toxic chemicals in general released into the environment.

Chromium adsorption isotherm measurements on a variety of geosorbents are often carried out using batch experiments by monitoring the aqueous phase chromium concentration in the absence and presence of the solid species. The concentration difference is then taken to be the amount adsorbed. Deng and Stone reported chromate adsorption isotherms on anatase ( $\text{TiO}_2$ )<sup>24</sup> as well as goethite and aluminum oxide.<sup>25</sup> The authors reported Langmuirian adsorption, with equilibrium constants for adsorption and desorption that were highest for goethite, followed by  $\text{TiO}_2$  and  $\text{Al}_2\text{O}_3$ . While these studies can be carried out using environmentally representative chromate concentration

levels as low as  $\mu\text{M}$ , the authors emphasize that the adsorption experiments rely on the assumption that chemical transformation of the adsorbate is negligible.<sup>24</sup> Chromate interaction with  $\text{Al}_2\text{O}_3$ ,  $\text{SiO}_2$ , goethite, and a variety of clays was also found to be efficient in studies by Buerge and Hug<sup>22</sup> in the order  $\text{Al}_2\text{O}_3 >$  goethite  $>$  clays (kaolinite, montmorillonite)  $>$   $\text{SiO}_2$ .

Geometries for adsorbed chromium species can be determined using X-ray spectroscopies.<sup>26</sup> For instance, Fitts et al. reported the formation of hydroxo-bridged Cr(III) dimers and higher-order polymers bound to  $\gamma\text{-Al}_2\text{O}_3$ ,<sup>27</sup> and Baron et al.<sup>6</sup> reported the formation of hydrated and hydroxylated adsorbate states in soils. Grossl et al.<sup>18</sup> and Fendorf et al.<sup>20</sup> reported that chromate formed monodentate, bidentate–binuclear, and bidentate–mononuclear surface complexes on goethite ( $\alpha\text{-FeOOH}$ ), suggesting both tetrahedral and hexagonal coordination of chromium by oxygen. Formation of these adsorbate structures was found to depend on surface coverage, and proposed binding models include both inner- and outer-sphere mechanisms.

In general, surface-specific approaches for studying chromium interaction with geosorbents are limited by relatively low sensitivities, and consequently most surface studies in the available literature are carried out using chromium concentrations that exceed the ones found in most contaminated and uncontaminated soils by several orders of magnitude. The EPA's maximum contaminant level goal for total chromium in drinking water is 0.1 mg/L (corresponding to a total chromium concentration level of  $2 \mu\text{M}$ ),<sup>28,29</sup> and chromium concentration levels at various waste sites in the states of New York, Colorado, and Michigan are found to be in the 0.1–1 mM regime.<sup>5</sup> Due to the nonlinear relationship between aqueous phase concentration and surface coverage for small aqueous phase concentrations,<sup>30</sup> the application of kinetic, thermodynamic, mechanistic, and structural information obtained from experiments that use high concentration levels is problematic. Thus, in the context of environmentally representative chromium concentrations approaching the EPA limit, our understanding of chromium adsorption isotherms on a variety of substrates remains qualitative.<sup>15,18–20,22,25,31</sup>

\* Email: geigerf@chem.northwestern.edu.

<sup>†</sup> Present address: Department of Chemistry, Columbia University, 3000 Broadway, New York, NY 1002.

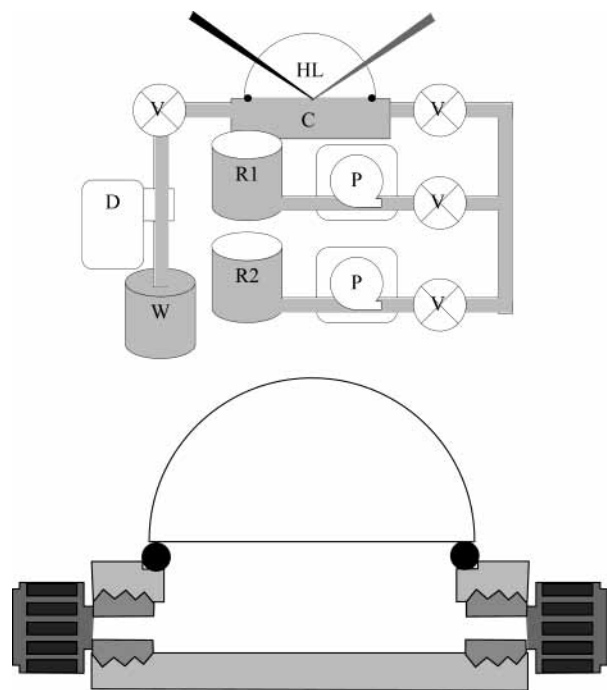


**Figure 1.** Dual pump flow system with hemispherical lens attached to the Teflon sample cell (top). Teflon flow cell with Swagelok fitting enlarged (bottom).

## II. Experimental Section

**Materials/Methods.** Since silicates are commonly found in the inorganic soil phase,<sup>23,32</sup> we have chosen the fused quartz/water interface as an initial heterogeneous system for our studies. In the natural environment, quartz is usually present in a less pristine form than the fused quartz samples employed in this work. However, we begin our studies on chromium binding to mineral oxide/water interfaces by using a simple heterogeneous system that can be expanded in chemical complexity, which is the subject of future work. After careful cleaning with Nochromix (Godax Laboratories) solution and rinsing with copious amounts of HPLC grade deionized water (VWR), the flat side of a 1" diameter fused quartz hemispherical lens (HL, ISP Optics) is placed over a custom-built Teflon flow cell (C) and held leak-tight using a Viton O-ring and a clamp (See Figure 1). The sample solutions are stored in liquid reservoirs (R1 and R2). The chromium-containing aqueous phase is flown across the interface using flow-controlled peristaltic pumps (P, Fisher). A second peristaltic pump for HPLC grade deionized water allows us to vary the chromate concentration in real time. A length of tubing between the sample cell and the point where both flows are combined ensures proper mixing of the sample solutions. Swagelok fittings are used for connecting the tubing and the cell.

Our dual-pump approach allows us to turn the solute flow on and off at a given time using Teflon on-off valves (V, Swagelok) while maintaining a constant overall flow rate. Simultaneously with the SHG surface measurements, the solute concentration is recorded in real time using a diode array UV-vis spectrometer (D, Ocean Optics, 185–850 nm). Potassium chromate salt (ICN Biomedicals) was used as received for preparing the aqueous chromate solutions. At the chromate concentrations used, the pH did not change, and no buffer was needed to maintain the aqueous phase at pH7. The pH was checked regularly with a pH meter. Standard sodium hydroxide and hydrogen chloride solutions were used to adjust the pH. The SHG intensity from surface-bound chromate did not change

upon replacing the aqueous phase with a  $10^{-3}$  M NaCl solution, indicating that in this concentration regime counterions did not replace the adsorbed chromate.

**Surface SHG.** Aqueous chromate displays electronic transitions in the UV-vis which originate from ligand-to-metal transitions.<sup>9,13,33–39</sup> Adsorbates with electronic resonances in the UV-vis range can be probed and identified directly at the surface using resonantly enhanced SHG.<sup>40–45</sup> In SHG, two photons of the same fundamental frequency are concertedly coupled into one photon at twice the frequency; i.e., light at a wavelength  $\lambda$  is converted into light at a wavelength  $\lambda/2$ . This nonlinear optical effect becomes important when high-intensity light fields (e.g., from lasers) are present in noncentrosymmetric media, including surfaces and interfaces.<sup>40–45</sup> The second-harmonic intensity,  $I_{\text{SHG}}$ , is related to the nonlinear susceptibility,  $\chi^{(2)}$ , of the medium. In centrosymmetric media, such as bulk water or bulk fused quartz,  $\chi^{(2)}$  is zero in the electric dipole approximation, and SHG is thus not allowed in centrosymmetric media. The interface between two bulk media, however, is noncentrosymmetric, and  $\chi^{(2)}$  of the interface is nonzero.

The second harmonic intensity  $I_{\text{SHG}}$  can be modeled as the product of the number density of molecules adsorbed on a surface and the second-order nonlinear molecular polarizability, averaged over all molecular orientations, according to

$$\sqrt{I_{\text{SHG}}} \sim \chi^{(2)} = N_{\text{ads}} \langle \alpha^{(2)} \rangle \quad (1)$$

Equation 1 shows that SHG can be used to perform kinetic studies of heterogeneous processes by monitoring the square-rooted SHG intensity, which is proportional to the number of adsorbed species at the interface, as a function of time.

The perturbation expansion for the second-order nonlinear molecular polarizability contains terms related to electronic transitions in the molecules and can be described by electric dipole transition terms

$$\alpha_{ijk}^{(2)} = -\frac{4\pi^2 e^3}{\hbar^2} \sum_{b,c} \frac{\langle a | \bar{\mu}_i | b \rangle \langle b | \bar{\mu}_j | c \rangle \langle c | \bar{\mu}_k | a \rangle}{(\omega - \omega_{ba} + i\Gamma_{ba})(2\omega - \omega_{ca} + i\Gamma_{ca})} + \dots \quad (2)$$

where  $\Gamma$  represents damping coefficients,  $\bar{\mu}_i$  is the electric dipole transition moment,  $a$ ,  $b$ , and  $c$  represent the ground, intermediate, and final state respectively, and the summation is over all excited states.<sup>40,46</sup> As  $\omega$  or  $2\omega$  (the frequency of the input light or the second harmonic frequency, respectively) approaches a natural resonance frequency of the adsorbate ( $\omega_{ba}$  or  $\omega_{ca}$ ), the second-order nonlinear molecular polarizability and the SHG efficiency increase. Thus, SHG allows for interface-specific spectroscopic studies.

**Laser System.** The SHG studies are carried out using a kHz 120 fsec regeneratively amplified Ti:Sapphire system (Hurricane, Spectra Physics) pumping an optical parametric amplifier containing a Type II BBO crystal (OPA-CF, Spectra Physics). For the present study, frequency doubling of the signal and sum frequency mixing of the signal and the residual pump from the OPA produce femtosecond probe light between 480 and 800 nm and allow for the collection of SHG surface spectra between 240 and 400 nm (3 nm bandwidth). The spot probed by the laser beam is approximately 50  $\mu\text{m}$  in diameter. The 580 nm reflection from the fused quartz/water interface is specular, which means that the substrate is optically flat, consistent with a surface roughness below 290 nm. Measurements of the SHG intensity obtained from the fused quartz/water interface as a function of pH reproduced the pH-dependent results of Ong et

al.<sup>47</sup> and Higgins et al.<sup>48</sup> and are consistent with a point of zero charge for the fused quartz/water interface between 2 and 3.5. We correct for laser output power fluctuations using SHG<sup>49–51</sup> reference lines, employing z-cut quartz reference samples (Boston Piezo-Optics). Substrate heating<sup>52</sup> is minimized by using femtosecond probe pulses and by probe light field attenuation below damage threshold via variable neutral density filters.<sup>51</sup> Quadratic power dependencies and spectral bandwidth of the nonlinear signals are verified regularly; departure from quadratic power dependence and the 3 nm spectral bandwidth for the SHG is observed at laser fluences above 8  $\mu\text{J}$ . Signal absorption by the aqueous phase is avoided by probing the liquid–solid interface from the fused quartz side at an angle of 60°, which is near the total internal reflection (TIR) angle for the quartz/water interface. Radiation from processes other than SHG is rejected using Schott filters and a monochromator (Monospec, TVC). The SHG signal is directed into a Hamamatsu photomultiplier tube (0.5 dark counts/s), preamplified, and the number of second harmonic photons is recorded versus time using a gated photon counter (Stanford Research Systems). Typical signal intensities are on the order of 0.01–0.1 counts per laser shot with our experimental setup and are independent of the bulk flow rate at a given sample concentration and pH.

A non-TIR geometry was used for a control experiment to verify that the results obtained with the near-TIR geometry were not biased by the choice of that geometry. In these experiments, a custom-built hemispherical quartz cell with an opening at the top was sealed tight with a Viton O-ring against a flat glass plate covered with Parafilm on which a fused quartz sample (Edmund Scientific) was placed. The probe laser was directed onto the sample from the aqueous phase at an incident angle of 60°, and the SHG signal was recorded in reflection mode. The results were identical to the ones obtained with the near-TIR geometry; the signal intensities, however, were lower by a factor of 3 to four.

### III. Results/Discussion

**Spectroscopic Characterization of Chromate at the Fused Quartz/Water Interface.** Before spectroscopically characterizing adsorbed chromate at the fused quartz/water interface, the SHG response of the neat fused quartz/water interface at pH 7 (no chromate present) was measured and found to be flat between 280 and 360 nm. This spectrum was recorded using the frequency-doubled signal beam from the OPA as the input and represents the nonresonant contribution of the neat quartz–water interface.

Figure 2a shows the SHG surface spectrum of chromate adsorbed to a fused quartz–water interface. The spectrum was obtained by scanning the fundamental frequency at constant pulse energy (1.5  $\mu\text{J}/\text{pulse}$ ) and by recording the SHG at the corresponding wavelength. According to eq 2, resonance enhancement of the SHG signal should occur once the SHG wavelength matches an electronic transition in the adsorbed species. The chromate concentration was held at  $5 \times 10^{-5}$  M and pH 7 and, on the basis of the chromate adsorption isotherm, corresponds to monolayer coverage (vide infra). During the collection of the spectrum, the chromate solution was flown over the fused quartz/water interface in a closed loop at a rate of 0.5 mL/s. Upon stopping the chromate flow, the SHG signal intensity did not change, indicating that mixing in the cell was complete. The p-in–p-out polarization combination was used in all experiments.

The SHG spectrum shown in Figure 2a displays a resonance centered at 290 nm and the beginning of a second resonance at

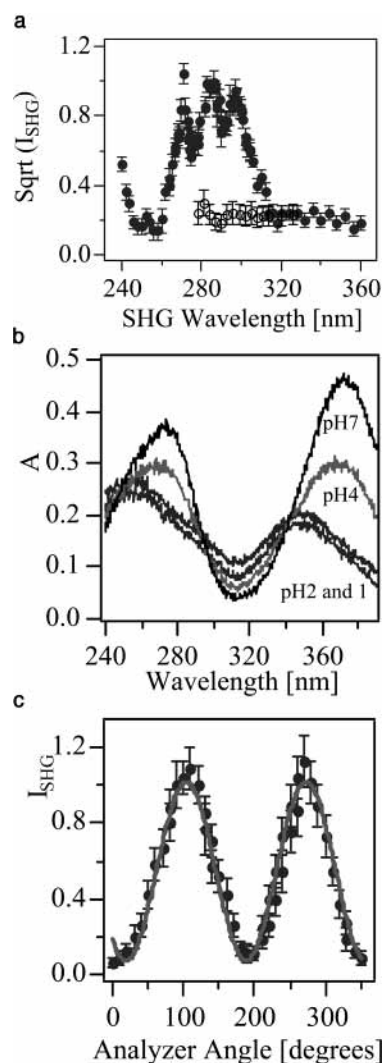


**Figure 2.** (a) Normalized surface SHG spectrum of a quartz–water interface at pH 7 (empty circles) and a quartz–water interface exposed to a  $5 \times 10^{-5}$  M  $\text{CrO}_4^{2-}$  solution at pH 7 (filled circles). The polarization combination is p-in/p-out. (b) Bulk absorption spectra of chromate solutions at pH 7, 4, 2, and 1. (c) SHG intensity as a function of analyzer angle (p-in). The quartz/water interface was in contact with a  $10^{-5}$  M chromate solution held at pH 7. The thick line is a sinusoidal fit to the data.

wavelengths below 240 nm. The 290 nm band in the SHG spectrum has an overall bandwidth that is comparable to the two ligand-to-metal transitions of chromate ions in bulk aqueous solution at pH >4, which occur at about 275 and 370 nm (see Figure 2b) with a measured absorption coefficient of  $3400(100)$   $\text{M}^{-1} \text{cm}^{-1}$  and  $4500(100)$   $\text{M}^{-1} \text{cm}^{-1}$ , respectively, at pH 7. Further, the SHG spectrum shown in Figure 2a appears to display some degree of fine structure in the 290 nm band.

Since the SHG intensity increases at smaller wavelengths but not at longer wavelengths, one could argue that the SHG spectrum represents the lower-energy ligand-to-metal transition of adsorbed chromate, and that the beginning of the peak at around 240 nm in the SHG spectrum could be due to the higher-energy ligand-to-metal transition of the adsorbed species. The apparent blue shift in the SHG spectrum compared to the lower-energy ligand-to-metal transition of chromate in aqueous solution at pH >4 would be consistent with a binding mechanism that involves (1) the chromate oxygen ligands and surface SiOH groups and/or (2) the formation of  $\text{HCrO}_4^-$  at the surface (below pH 4, chromate in aqueous solution exists in the



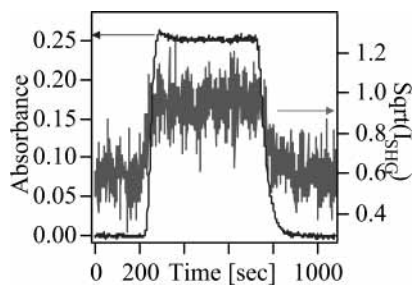


**Figure 3.** Square-rooted and normalized SHG vs time trace (right) and  $\text{CrO}_4^{2-}$  absorbance vs time trace at 372 nm (left) for a  $\text{CrO}_4^{2-}$  adsorption and desorption experiment.  $\lambda_{\text{SHG}} = 290$  nm; p-in/p-out. The SHG signals are on the order of 0.01 and 0.1 counts per shot.

protonated form, showing a 20 nm blue shifted ligand-to-metal transition with respect to chromate at  $\text{pH} > 4$ , see Figure 2b). Studies focusing on the pH dependence of the SHG surface spectra and extended wavelength studies are currently underway to further investigate the spectroscopy of chromate adsorbed to the quartz–water interface.

A polarization analysis of the SHG obtained from the quartz/water interface in contact with a  $1 \times 10^{-5}$  M chromate solution held at pH 7, shown in Figure 2c, indicates that the SHG signals obtained from chromate adsorbed to the quartz–water interface are well polarized. The chromate surface coverage in this experiment was below a monolayer (vide infra). The polarization results shown in Figure 2c are expected and confirm that an s-polarized SHG signal is forbidden when driven by a p-polarized light field in uniaxial surface systems, suggesting that in this experiment chromate is isotropically adsorbed to the quartz–water interface. Examination of the null-angles obtained from these measurements allows us to gain additional orientational information for the adsorbed chromate,<sup>53</sup> which will be addressed in future studies.

**Kinetics of Chromate Interaction with the Fused Quartz/Water Interface.** Shown as the right trace in Figure 3 is an SHG versus time trace for chromate adsorbing from the aqueous phase to a quartz/water interface ( $[\text{CrO}_4^{2-}] = 1 \times 10^{-5}$  M) with consecutive desorption. The interface was probed at 580 nm, and the corresponding SHG at 290 nm was recorded, resulting in SHG resonance enhancement due to one of the ligand-to-metal transitions in  $\text{CrO}_4^{2-}$  in the near UV (see Figure 2a). Using our dual-pump flow system, water was flown over the fused quartz/water interface at a rate of 0.4 mL/s. At 200 s, the water flow was stopped, and simultaneously the chromate flow was started at the same flow rate such that the overall flow rate did not change. The square-rooted SHG signal is observed to increase and reaches steady-state at  $\sim 300$  s at a signal level  $\sim 2$  times above the background from the neat quartz/water interface. On the basis of the SHG surface spectrum shown in Figure 2a and the increase of the  $\text{CrO}_4^{2-}$  absorbance measured in the solution exiting the sample cell (left trace in Figure 3), the SHG signal increase is attributed to chromate adsorption at the quartz/water interface, consistent with eq 1. Figure 3 also shows that chromate adsorption is completely reversible: Once the chromate flow is halted and the aqueous phase replaced with plain water, the square-rooted SHG signal decays to its original background level, indicating that all chromate has desorbed from the interface. This is consistent with the general notion that, dependent on environmental conditions and type of sorbent, hexavalent chromium is mobile in the environment.

The kinetic trace shown in Figure 3 indicates that chromate adsorption and desorption occurs slowly and over the course of several minutes. This time scale indicates that chromate

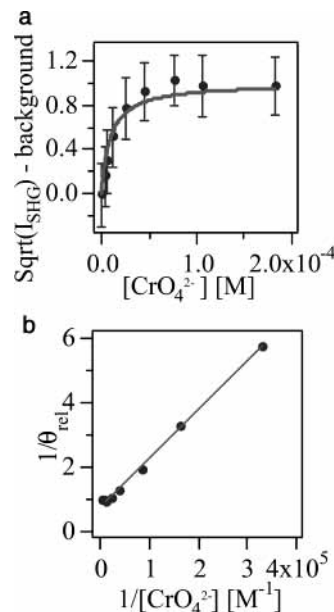


**Figure 4.** (a) Adsorption isotherm of  $\text{CrO}_4^{2-}$  at the quartz–water interface at pH 7 bulk solution. (b) Inverse  $\text{CrO}_4^{2-}$  surface coverage vs inverse chromate concentration.

diffusion from the bulk to the solid–liquid interface is important, and this important issue will be addressed in future work.

**Thermodynamics of Chromate Adsorbed to the Fused Quartz/Water Interface.** Figure 4a shows the isotherm for chromate adsorption to the water/quartz interface at room temperature. The solution was held at pH 7, and the chromate concentration ranged from  $3 \times 10^{-6}$  to  $2 \times 10^{-4}$  M. The background-subtracted and square rooted SHG signal is proportional to the number density of adsorbates (vide supra). Figure 4a shows that monolayer coverage is reached at  $5 \times 10^{-5}$  M, and that at the concentration approaching the EPA concentration limit ( $10^{-6}$  M), the chromate surface coverage reaches zero. As has recently been discussed by Simpson and Rowlen,<sup>54,55</sup> orientation effects on the SHG signals are important in many heterogeneous systems when carrying out adsorption isotherms or kinetic studies, and we will address this subject in future studies.

The chromate adsorption isotherm may be analyzed in terms of a simple Langmuir adsorption model, in which the inverse of the relative surface coverage is plotted as a function of inverse chromate concentration, shown in Figure 4b. From the slope of the resulting straight line, the free energy of chromate adsorption to the quartz–water interface can be determined according to

$$[d(1/\theta)/d(1/[\text{CrO}_4^{2-}])]^{-1} = \frac{1}{55.5\text{M}} \exp(-\Delta G_{\text{ads}}^{\circ}/RT) \quad (3)$$

(a molarity of 55.5 M is used for the aqueous solution).<sup>30</sup> With a slope of  $1.54(2) \times 10^{-5} \text{ M}^{-1}$ , corresponding to an equilibrium adsorption constant of  $3.6(1) \times 10^6 \text{ M}^{-1}$ , the free energy of chromate adsorption to the quartz–water interface is found to be  $38(1) \text{ kJ/mol}$  at room temperature and pH 7, consistent with the formation of 2–3 hydrogen bonds and a weak physisorption process governing the interaction of chromate with quartz–water interfaces. Given our observation that chromate adsorption and desorption is fully reversible and given the relatively low free energy for chromate binding consistent with the formation of two to three hydrogen bonds, the interaction of chromate with the fused quartz/water interface appears to be governed by a physisorption process via hydrogen bonding. The binding

mechanism might thus be one dominated by the interaction of the chromate oxygen ligands with the interface, consistent with the notion that the formation of outer-sphere complexes can be important for chromate binding in certain soil environments.

We also recorded the chromate adsorption isotherm at pH 4 and found it to be similar to the isotherm obtained at pH 7, with a free energy of adsorption of chromate to the quartz/water interface of 38(1) kJ/mol at pH 4 as well. These free energies are slightly higher than the ones reported for chromate adsorption onto aluminum oxide, goethite and titanium dioxide by Deng and Stone,<sup>25</sup> and this difference is attributed to the difference in the systems investigated, i.e., the fact that macroscopic flat interfaces, versus colloid particle surfaces, are studied here. Adsorption experiments carried out at pH 10 showed no change in the SHG signal when chromate was present in the aqueous phase; i.e., binding of the doubly negatively charged chromate to the quartz/water interface was not observed. This is consistent with the fact that quartz/water interfaces have a point of zero net proton charge between pH 1 and 3,<sup>23,56,57</sup> with SiO<sup>-</sup> surface coverage increasing with increasing pH.<sup>23,58</sup>

**Environmental Significance.** The present study shows that nonlinear optical spectroscopies can be applied to study the interaction of toxic metals of environmental concern with water/quartz interfaces. The approach yields surface-specific spectroscopic, kinetic, and thermodynamic data, which may be used for modeling toxic metal migration in contaminated soils. In the case of chromate, the experiments can be carried out with submonolayer sensitivity, and in a chromate concentration range that is environmentally significant (as low as 10<sup>-6</sup> M, i.e., the EPA limit for chromium). Furthermore, chromate adsorption and desorption processes can be followed in real time, and the experiments can be carried out over a range of environmentally relevant pH values.

Future studies will address the effect that inorganic and organic impurities located at the quartz surface have on chromium binding. These studies appear especially useful in light of the fact that chromate may not always be mobile, depending on environmental conditions and type of sorbent.<sup>20</sup> Further, we plan to study redox reactions that chromate can undergo at water/mineral oxide interfaces, paying particular attention to the important role that coadsorbed organic and inorganic species have in the heterogeneous chemistry of chromium in contaminated environments.

#### IV. Conclusions

Second-harmonic generation measurements on the adsorption and desorption of chromate at fused quartz/water interfaces were carried out. Adsorbed chromate is spectroscopically identified by a two-photon resonance of one of its ligand-to-metal charge transfer bands with the fundamental of the probe laser. Chromate binding to the fused quartz-water interface is found to be completely reversible, consistent with the general notion that chromate is highly mobile in the environment. Equilibrium adsorption isotherms appear Langmuirian and result in a free energy of adsorption of 38(1) kJ/mol at pH 4 and 7, consistent with the formation of two to three hydrogen bonds upon chromate adsorption to the fused quartz/water interface. The chromate surface coverage approaches a monolayer at a chromate concentration around 5 × 10<sup>-5</sup> M and approaches zero at chromate concentrations around 10<sup>-6</sup> M.

**Acknowledgment.** K.A.G. acknowledges a Northwestern University Summer Research Fellowship for Undergraduates.

B.M.W. acknowledges a Columbia University Langmuir Fellowship. We gratefully acknowledge helpful comments from the reviewers as well as donations from Spectra Physics.

#### References and Notes

- (1) Kavanaugh, M. C. *Alternatives for Groundwater Cleanup*; Academic Press: Washington, DC, 1994.
- (2) Rubin, E. S. *Environ. Sci. Technol.* **1999**, *33*, 3062.
- (3) Ribeiro, A. B.; Mateus, E. P.; Ottosen, L. M.; Bech-Nielsen, G. *Environ. Sci. Technol.* **2000**, *34*, 784.
- (4) Helsen, L.; Van den Bulck, E. *Environ. Sci. Technol.* **2000**, *34*, 2931.
- (5) Nriagu, J. O.; Nieboer, E. *Chromium in the Natural and Human Environments*; John Wiley & Sons: New York, 1988.
- (6) Baron, D.; Palmer, C. D.; Stanley, J. T. *Environ. Sci. Technol.* **1996**, *30*, 964.
- (7) Arfsten, D. P.; Aylward, L. L.; Karch, N. J. Chromium. In *Immunotoxicology of Environmental and Occupational Metals*; Zelikoff, J. T., Thomas, P. T., Eds.; Taylor & Francis Inc.: Bristol, PA, 1998.
- (8) Katz, S. A.; Salem, H. *The Biological and Environmental Chemistry of Chromium*; VCH: New York, 1994.
- (9) Greenwood, N. N.; Earnshaw, A. *Chemie der Elemente*; VCH Verlagsgesellschaft: Weinheim, 1990.
- (10) Goldman, L. R.; Lanphear, B. P. *Science* **1998**, *282*, 1823.
- (11) Goyer, R. A.; Klaassen, C. D.; Waalkes, M. P. *Metal Toxicology*; Academic Press: New York, 1995.
- (12) Pattison, D. I.; Davies, M. J.; Levina, A.; Dixon, N. E.; Lay, P. A. *Chem. Res. Toxicol.* **2001**, *14*, 500.
- (13) Holleman, A. F.; Wiberg, N. *Lehrbuch der Anorganischen Chemie*; W. de Gruyter: Berlin, 1985.
- (14) Chromium. In *National Research Council (US): Committee on Biologic Effects of Atmospheric Pollutants*; National Academy of Sciences: Washington, DC, 1974; p 125.
- (15) Jardine, P. M.; Fendorf, S. E.; Mayes, M. A.; Larsen, I. L.; Brooks, S. C.; Bailey, W. B. *Environ. Sci. Technol.* **1999**, *33*, 2939.
- (16) August, E. E.; Mcknight, D. M.; Hrcncir, D. C.; Garhart, K. S. *Environ. Sci. Technol.* **2002**, *36*, 3779.
- (17) Tokunaga, T. K.; Wan, J.; Firestone, M. K.; Hazen, T. C.; Schwartz, E.; Sutton, S. R.; Newville, M. *Environ. Sci. Technol.* **2001**, *35*, 3169.
- (18) Grossl, P. R.; Eick, M.; Sparks, D. L.; Goldberg, S.; Ainsworth, C. C. *Environ. Sci. Technol.* **1997**, *31*, 32.
- (19) Weng, C. H.; Huang, C. P.; Allen, H. E.; Leavens, P. B.; Sanders, P. F. *Environ. Sci. Technol.* **1996**, *30*, 371.
- (20) Fendorf, S.; Eick, M. J.; Grossl, P.; Sparks, D. L. *Environ. Sci. Technol.* **1997**, *31*, 315.
- (21) Loyaux-Lawniczak, S.; Refait, P.; Ehrhardt, J.-J.; Lecomte, P.; Genin, J.-M. *Environ. Sci. Technol.* **2000**, *34*, 438.
- (22) Buerge, I. J.; Hug, S. J. *Environ. Sci. Technol.* **1999**, *33*, 4285.
- (23) Langmuir, D. *Aqueous Environmental Geochemistry*; Prentice-Hall: Englewood Cliffs, NJ, 1997.
- (24) Deng, B.; Stone, A. T. *Environ. Sci. Technol.* **1996**, *30*, 463.
- (25) Deng, B.; Stone, A. T. *Environ. Sci. Technol.* **1996**, *30*, 2484.
- (26) Weckhuysen, B. M.; Wachs, I. E.; Schoonheydt, R. A. *Chem. Rev.* **1996**, *96*, 3327.
- (27) Fitts, J. P.; Brown, G. E.; Parks, G. A. *Environ. Sci. Technol.* **2000**, *34*, 5122.
- (28) U.S. EPA. *National Primary Drinking Water Standards*, 2002.
- (29) Buonicore, A. J. *Cleanup Criteria for Contaminated Soil and Groundwater*; ASTM: West Conshohocken, PA, 1996.
- (30) Adamson, A. W. *Physical Chemistry of Surfaces*, 5th ed.; John Wiley & Sons: New York, 1990.
- (31) Rai, D.; Eary, L. E.; Zachara, J. M. *Sci. Total Environ.* **1989**, *86*, 15.
- (32) Evangelou, V. P. *Environmental Soil and Water Chemistry*; John Wiley & Sons: New York, 1998.
- (33) Pourbaix, M. *Atlas of Electrochemical Equilibria*; Pergamon Press: New York, 1966.
- (34) Shriver, D. F.; Atkins, P. W.; Langford, C. H. *Inorganic Chemistry*; Oxford University Press: Oxford, 1991.
- (35) Cotton, F. A.; Wilkinson, G.; Murillo, C. A.; Bochmann, M. *Advanced Inorganic Chemistry*, 6th ed.; John Wiley & Sons: New York, 1988.
- (36) DeArmond, K.; Forster, L. S. *Spectrochim. Acta* **1963**, *19*, 1393.
- (37) Bailey, N.; Carrington, A.; Lott, K. A.; Symons, M. C. R. *J. Chem. Soc.* **1960**, 290.
- (38) Mishra, H. C.; Symons, M. C. R. *J. Chem. Soc.* **1962**, 4411.
- (39) Gustin, V. K.; Sweet, T. R. *Anal. Chem.* **1961**, *33*, 1942.
- (40) Shen, Y. R. *The Principles of Nonlinear Optics*; John Wiley & Sons: New York, 1984.
- (41) Shen, Y. R. *Nature* **1989**, *337*, 519.
- (42) Eisenthal, K. B. *Chem. Rev.* **1996**, *96*, 1343.

- (43) Shen, Y. R. *Surf. Sci.* **1994**, 299/300, 551.
- (44) Eienthal, K. B. Equilibrium and dynamic processes at interfaces by second harmonic and sum frequency generation. In *Annual Review of Physical Chemistry*; Strauss, H. L., Babcock, G. T., Leone, S. R., Eds.; Annual Reviews Inc: Palo Alto, CA, 1992; Vol. 43, p 627.
- (45) Heinz, T. F. *Nonlinear Surface Electromagnetic Phenomena*; Elsevier Publishers: 1991.
- (46) Boyd, R. W. *Nonlinear Optics*; Academic Press: New York, 1992.
- (47) Ong, S.; Zhao, X.; Eienthal, K. B. *Chem. Phys. Lett.* **1992**, 191, 327.
- (48) Higgins, S. R.; Stack, A. G.; Knauss, K. G.; Eggleston, C.; Jordan, G. Probing molecular-scale adsorption and dissolution-growth processes using nonlinear optical and scanning probe methods suitable for hydrothermal applications. In *Water-Rock Interactions, Ore Deposits, and Environmental Geochemistry: A Tribute to David A. Crerar*; Hellmann, R. a. W., S. A., Ed.; Special Publication No. 7; The Geochemical Society: 2002.
- (49) Geiger, F. M.; Tridico, A. C.; Hicks, J. M. *J. Phys. Chem. B* **1999**, 103, 8205.
- (50) Geiger, F. M.; Pibel, C. D.; Hicks, J. M. *J. Phys. Chem. A* **2001**, 105, 4940.
- (51) Sandrock, M. L.; Pibel, C. D.; Geiger, F. M.; Foss, C. A. *J. Phys. Chem. B* **1999**, 103, 2668.
- (52) Hicks, J. M.; Urbach, L. E.; Plummer, E. W.; Dai, H. L. *Phys. Rev. Lett.* **1988**, 61, 2588.
- (53) Heinz, T. F. Nonlinear Optics of Surfaces and Adsorbates. Ph.D. dissertation, University of California, Berkeley, 1982.
- (54) Simpson, G. J.; Rowlen, J. L. *Anal. Chem.* **2000**, 72, 3407.
- (55) Simpson, G. J.; Rowlen, J. L. *Anal. Chem.* **2000**, 72, 3399.
- (56) Koretsky, C. *J. Hydrol.* **2000**, 230, 127.
- (57) Stumm, W.; Morgan, J. J. *Aquatic Chemistry*, 3rd ed.; Wiley-Interscience: New York, 1996.
- (58) Duval, Y.; Mielczarski, J. A.; Pokrovsky, O. S.; Mielczarski, E.; Ehrhardt, J. J. *J. Phys. Chem. B* **2002**, 106, 2937.